

WORCESTER POLYTECHNIC INSTITUTE

Biophysical Characterization of Diacylglycerol Pyrophosphate

A Major Qualifying Project Report:
submitted to the Faculty of the
WORCESTER POLYTECHNIC INSTITUTE
in partial fulfillment of the requirements for the
Degree of Bachelor of Science

Justin Siemian
4/25/2013

Approved:

Dr. Arne Gericke, Project Advisor

Abstract

Diacylglycerol pyrophosphate (DGPP), a phosphorylated form of phosphatidic acid (PA), gained attention due to its role as a signaling lipid. In plants, DGPP is virtually absent in non-stimulated cells but its concentration increases within minutes in response to various stimuli including osmotic stress and pathogen attack. While genetic manipulation of DGPP levels has shown that DGPP has a functional role in stress responses in plants, it is unclear to date what its molecular function is and how it exerts its effects. To help better characterize the functions of PA and DGPP, this study examined the lipids in pH 4 through 11 by infrared spectroscopy, and found that the pure DOPA multilamellar vesicles deprotonate to the PO_3^{2-} species at lower pH than pure DGPP multilamellar vesicles, which is different than what has been found in previous studies. This study elucidated the ionization state and stretching frequencies of each lipid over the physiological pH range.

Introduction

Biological membranes are vital to the function of cells in all organisms, acting as selective barriers within or around a cell. Influenced heavily by membrane proteins, biomembrane structure and function is also affected by their diverse lipid composition. It is well known that lipids that form a hexagonal phase upon full hydration add a negative curvature stress to biomembranes which facilitates membrane bending, for example membrane fusion and protein insertion. In contrast, lipids that form a micellar phase (“detergents”) add a positive curvature stress to membranes and were shown to prevent membrane fusion. While the phase behavior and structure of many membrane lipids have been characterized in great detail (Gennis, 1989; Marsh, 2012), much still remains to be learned to fully appreciate the defining properties of membrane lipids and to understand the reason for the immense diversity of lipids found in biological membranes. Specifically, the function and properties of lipids that

serve as important signaling molecules and occur in membranes in small and quickly changing concentrations require further research (Strawn, 2012).

One such lipid-signaling molecule that has emerged in all eukaryotes is phosphatidic acid (PA). So far, it is known that PA is involved in mitogenic signaling, vesicular trafficking, and the oxidative burst in animals (Ktistakis et al., 2003; Rizzo et al., 2002). In plants, PA plays a role in stress signaling and is generated rapidly in response to salinity, cold, wounding, and pathogen attack. Data from plants, mammals, and yeast indicated that PA formation functions as a membrane-localized signal, affecting downstream responses by binding specific protein targets including protein kinases and phosphatases as well as proteins involved in vesicular trafficking (Stace and Ktistakis, 2006; Testerink and Munnik, 2011). Further, because of its small polar headgroup that adds negative charge and curvature to the bilayer, PA formation significantly affects membrane architecture, possibly reducing the energy barrier for vesicle fission and fusion even without interaction with proteins (Roth, 2008).

Stress induced increases in plants are always transient; PA levels increase within seconds to minutes after stimulation but also decrease rapidly, likely enabling the plant to respond to a new stimulus (van Schooten et al., 2006). Several pathways have been identified that serve to attenuate the PA signal (Testerink and Munnik, 2011). One such pathway is the phosphorylation of PA to diacylglycerol pyrophosphate (DGPP) by PA kinase (PAK) (Figure 1).

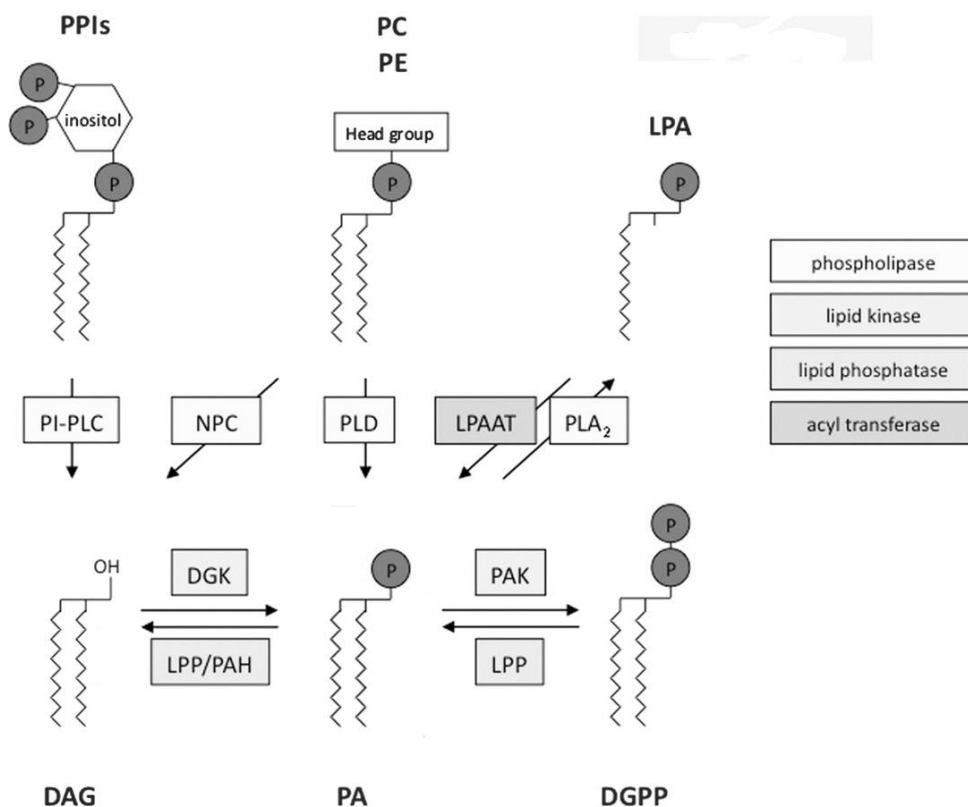


Figure 1: Overview of PA formation and degradation in plants. Abbreviations: PPIs; phosphatidylinositol lipids, PC; phosphatidylcholine, PE; phosphatidylethanolamine, LPA; lyso-PA, PI-PLC; PPI-hydrolysing phospholipase C, NPC; non-specific PLC, PLD; phospholipase D, LPAAT; LPA acyltransferase, PLA₂; phospholipase A₂, DAG; diacylglycerol, DGK; DAG kinase, LPP; lipid phosphate phosphatase, PA; phosphatidic acid, PAH; PA hydrolase, PAK; PA kinase, DGPP; diacylglycerol pyrophosphate. Figure adapted from Testerink and Munnik, 2011.

Present only in small amounts under normal conditions, DGPP levels are significantly raised upon hyperosmotic stress treatment (Pical et al., 1999; Munnik et al., 2000; Darwish et al., 2009), elicitation by both pathogenic and beneficial microorganisms (van der Luit et al., 2000; de Jong et al., 2004; den Hartog et al., 2001, 2003), and in response to the plant stress hormone abscisic acid (ABA) (Katagiri et al., 2005; Zalejski et al., 2005). Every condition where DGPP formation has been found was preceded by a transient increase in PA (van Schooten et al., 2006). While labeling experiments have shown that DGPP is synthesized by (beta) phosphorylation of PA, the gene encoding PAK activity has not yet been discovered, preventing genetic analysis of this pathway. On the other hand, DGPP can be

dephosphorylated to PA by the enzyme DGPP phosphatase (DPP), to which four genes have been linked thus far in *Arabidopsis thaliana* (Jeanette et al., 2010).

Studies have shown that DGPP formation is fast, starting 1 to 20 minutes after stimulation, and levels remained elevated for the duration of most experiments. In some cases, however, clear decreases were observed, implying the presence of an enzyme that turns over DGPP (den Hartog et al., 2001, 2003; van der Luit et al., 2000; Munnik et al., 2000; Pical et al., 1999; Zalejski et al., 2005; Latijnhouwers et al., 2002). The gene for this enzyme, called DGPP phosphatase (DPP), has been cloned from *S. cerevisiae* (Toke et al., 1998, 1998), *E. coli* (Dillon et al., 1996), and *A. thaliana* (Pierrugues et al., 2001). One DPP-encoding gene from *A. thaliana* was upregulated by treatment with the G-protein activator mastoparan and the elicitor harpin, agonists known to trigger DGPP formation. This was the first suggestion that DGPP levels may be also regulated at the level of gene expression in plants (van Schooten et al., 2006). The discovery of DPP implies that DGPP is not simply an inactivated form of PA, since DGPP levels are regulated as well.

Functional Role of DGPP in plants: Defining molecular properties

The current understanding of DGPP formation and degradation in plants as well as its molecular function is incomplete. Recent physicochemical studies of PA have led to the electrostatic-hydrogen bond switch model, which has been important in explaining some of its physiological functions. Experiments that examine the physicochemical state are likely necessary to understanding the physiology of this unusual lipid (Strawn et al., 2012). It has been shown that the ionization properties of the DGPP phosphomonoester mimic those of PA (follow the electrostatic-hydrogen bond switch model), suggesting the ability of DGPP to interact with cationic protein domains and possibly possessing unique signaling functions (Strawn et al., 2012). However, unlike PA, DGPP is not a cone-shaped lipid and thus cannot impart a negative membrane curvature, which would facilitate the insertion of hydrophobic

protein domains into the membrane. This is expected to have significant implications for the proteins that bind DGPP (Strawn et al., 2012). Strawn et al. propose that at physiological pH and salt concentration DGPP is a membrane-stabilizing lipid, contributing negligible curvature to a membrane, while PA is a membrane destabilizer.

The presence of two phosphates in DGPP could also significantly change the orientation and position of the phosphomonoester in the lipid headgroup-acyl chain interface (Strawn et al., 2012). With two phosphate groups stacked on top of each other, the phosphomonoester of DGPP is able to penetrate much farther toward the aqueous phase than the phosphomonoester of PA and is likely to experience a much larger dielectric constant, resulting in a lower pK_{a2} (Cevc, 1990; Tocanne and Teissie, 1990). This suggests that the phosphomonoester group of DGPP carries a more negative charge than the phosphomonoester group of PA, favoring the interaction with cationic protein domains, potentially resulting in the displacement of a PA bound protein with DGPP (Strawn et al., 2012). However, since DGPP is a membrane stabilizing phospholipid, the displacement of the protein from PA to DGPP might mean, strangely, that the protein loses affinity for the membrane, thus turning off a PA signal. Thus, the charge and packing properties of DGPP might work together in attenuating the PA signal (Strawn et al., 2012).

Two possibilities for the mechanism of DGPP action are likely: DGPP may function through the activation/recruitment of effector proteins by direct interaction and/or by a modulation of membrane properties such as packing, curvature, and electrostatics (Zalejski et al., 2005). It is of great importance, therefore, to first understand the interfacial packing and electrostatic behavior of this bioactive lipid as well as the interaction of this molecule with its precursor (Villasuso et al., 2010).

IR Spectra of Phosphorous Lipids

The overall goal of this study was the assignment of the phosphate band modes of the phosphorous lipids Dioleoyl PA and DGPP. As the spectra of these phosphorous lipids can be complex with subtle shifts due to pH changes, monomethyl phosphate (MMP) spectra from a separate study (Dawson, 2002) were used to assign the modes in the basic band pattern and to study the pH-dependent behavior of the phosphomonoester group. The one and two negative charges of the phosphomonoester group are widely agreed upon to be delocalized over two and three oxygen atoms, respectively.

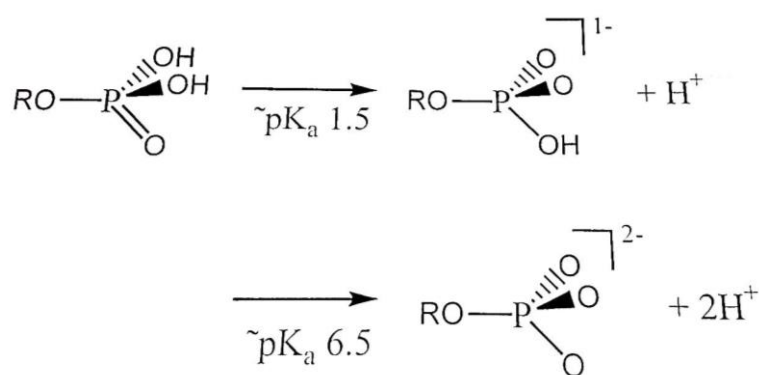


Figure 2: Ionic species of a general phosphomonoester (Adapted from Dawson, 2002).

Figure 2 shows the respective pK_a values near pH 1.5 and 6.5; the exact values depend on the chemical nature of the residue R (Dawson, 2002). Figure 3 shows the pH dependent changes of the phosphate stretching band pattern when changing the pH from 1.5 to 10.0. This pH range shows the subtle spectral changes as the initially neutral species becomes increasingly deprotonated and forms initially a single negatively and eventually double negatively charged monophosphate (Dawson, 2002).

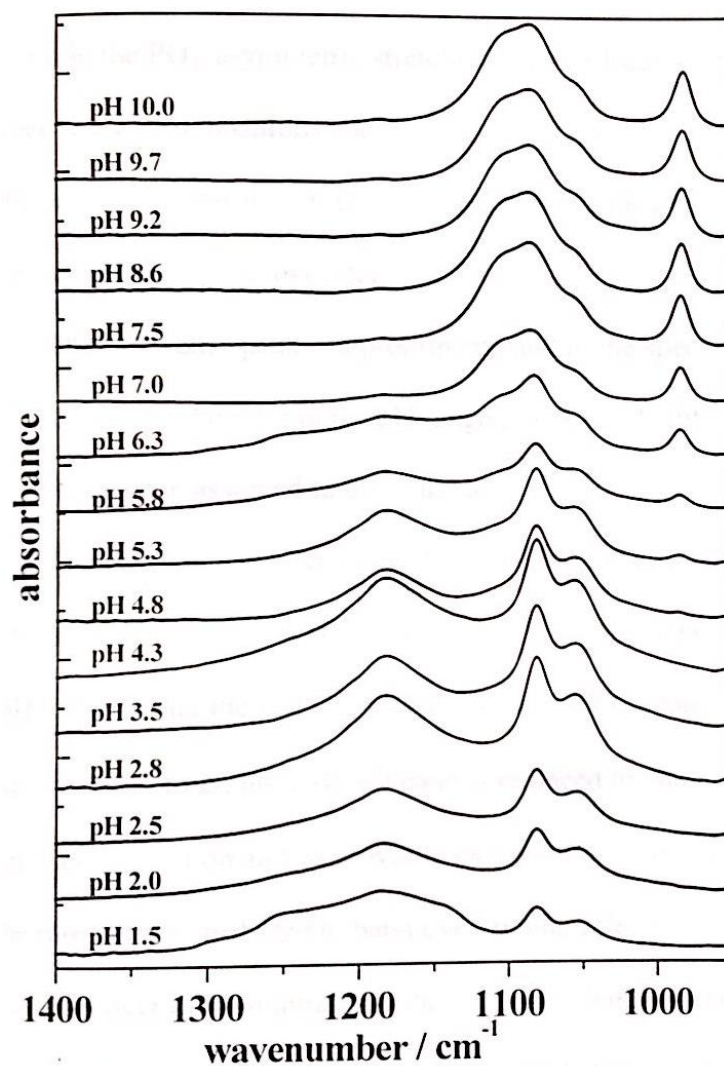


Figure 3: pH Dependent IR spectra of monomethyl phosphate

(Reproduced from Dawson, 2002 with permission from Gericke).

The pH dependent infrared spectroscopic analysis of monomethylphosphate (MMP) by Dawson yielded the following results: Beginning at pH 5.3, a peak centered at 984 cm^{-1} is observed that is increasing with increasing pH until it reaches a constant value around pH 7.0. Based on the pH range of its appearance and its dependence on pH, this peak is generally considered to be the PO_3^{2-} symmetric stretching vibration band (Shimanouchi et al., 1964; Thomas et al., 1970; Tsuboi, 1957). The corresponding PO_3^{2-} asymmetric stretching mode of the phosphomonoester is generally found in the $1055\text{-}1140\text{ cm}^{-1}$ range (Tsuboi, 1957). For MMP, two pH-dependent peaks are observed at 1087 and

1105 cm^{-1} in the pH range 1.5-10.0 and 5.8-10.0, respectively. Their assignment has been subject to some controversy, since both symmetric PO_2^- and asymmetric PO_3^{2-} vibrational modes are found in this spectral range (Dawson, 2002).

Two pH dependent peaks are present in the MMP spectra in the pH 1.5 to 6.0 (single negatively charged) range. The PO_2^- symmetric stretching mode is observed at 1081 cm^{-1} while the PO_2^- asymmetric stretching mode is observed at 1182 cm^{-1} (Dawson, 2002). A peak at 1250 cm^{-1} is prominent at pH 1.5 and exists as a slight shoulder from pH 2.0 to 4.3. The P=O stretching vibration has been assigned to this band (Thomas et al., 1964). The band found at 1052-1055 cm^{-1} varies only slightly in position and intensity with pH. This peak is part of a broad band envelope that contains either the $\nu_a(\text{PO}_3^{2-})$ bands or the $\nu_s(\text{PO}_2^-)$ band, depending on the pH value. As protonation changes from single protonated (1- charge) to unprotonated (2- charge), the $\nu_s(\text{PO}_2^-)$ is replaced by the $\nu_a(\text{PO}_3^{2-})$ band, which show differences in position and band width. Thus, the observed shift of the 1055 cm^{-1} band can likely be attributed to band overlapping (Dawson, 2002). Dawson tentatively assigned this peak as a C-O stretching mode.

Goals of This Study

As made apparent from the background, it is expected that DGPP will carry a larger negative charge than PA at an equivalent pH level, which would cause DGPP to interact more favorably with cationic protein domains. Thus, the first goal of this study is to determine whether or not the pyrophosphate group (specifically the phosphomonoester) actually deprotonates to 2- at a lower pH than DOPA. Analyzing these lipids by infrared spectroscopy over a pH 4-12.5 range will help to elucidate this. A secondary goal of this study is to assign definitive band positions to all of the bands found in the spectra produced by each lipid based on their trends in response to increasing pH. In addition to the Dawson study, other publications that examined ATP, ADP (Barth, 1995, 1998), and a variety of other

phosphate-containing molecules (Shimanouchi, 1960) via infrared spectroscopy were used to assign vibrational modes to specific wavenumbers.

Experimental Procedures

Diacylglycerol Pyrophosphate (diammonium salt; DGPP) and 1,2-dioleoyl-*sn*-glycero-3-phosphate (monosodium salt; DOPA) were purchased from Avanti Polar Lipids (Alabaster, AL, USA). Both lipids were dissolved in chloroform-methanol (2:1, v/v) to a final concentration of 1 mg/mL, and were used as they were received from Avanti. Water used in experiments was of HPLC grade and purchased from Fischer Scientific. All buffers (HEPES, MES, CHES) were at least of enzyme grade. NaCl was of ACS grade.

Sample preparation

Lipids were stored in chloroform/methanol (2:1) stock solutions. Multilamellar vesicles were prepared by drying appropriate amounts of the stock solutions in a stream of dry nitrogen. This drying process was carried out as quickly as possible at slightly elevated temperatures ($\approx 50^\circ\text{C}$). Subsequently, the samples were kept overnight in high vacuum at $45\text{--}50^\circ\text{C}$. Lipid samples were resuspended by vortexing three times for 60 s, with 5 minutes between each vortex. The lipid film was resuspended in buffer of the appropriate pH. Buffers used were: 20 mM Citric Acid, 30 mM MES $4 < \text{pH} < 6$, 10 mM HEPES $7 < \text{pH} < 8$, 50 mM CHES $9 < \text{pH} < 11$, and contained 100 mM NaCl.

Infrared Spectroscopy: equipment and parameters

FT-IR experiments were performed with a Bruker Tensor 27 Spectrometer (Billerica, MA) equipped with a medium band MCT detector. Interferograms were collected at 4 cm^{-1} (1000 scans), apodized with the Blackman-Harris function, and Fourier transformed with two levels of zero filling to yield spectra encoded at 1 cm^{-1} intervals. Lipid samples were sandwiched between two BaF₂ windows

(25 μm poly(tetrafluoroethylene) spacer) and placed in a cell holder. After completion of the lipid IR experiment, an equivalent volume of appropriate buffer was used to obtain a matched IR baseline that was obtained for the lipid sample. The spectra were processed by subtracting the buffer spectrum from the lipid spectrum using OPUS software. The positions of the $\text{PO}_2^-/\text{PO}_3^{2-}$ vibration bands were determined by calculating the second derivative followed by a center-of-mass peak pick algorithm. This typically results in a peak position accuracy of $\pm 0.1 \text{ cm}^{-1}$.

Results

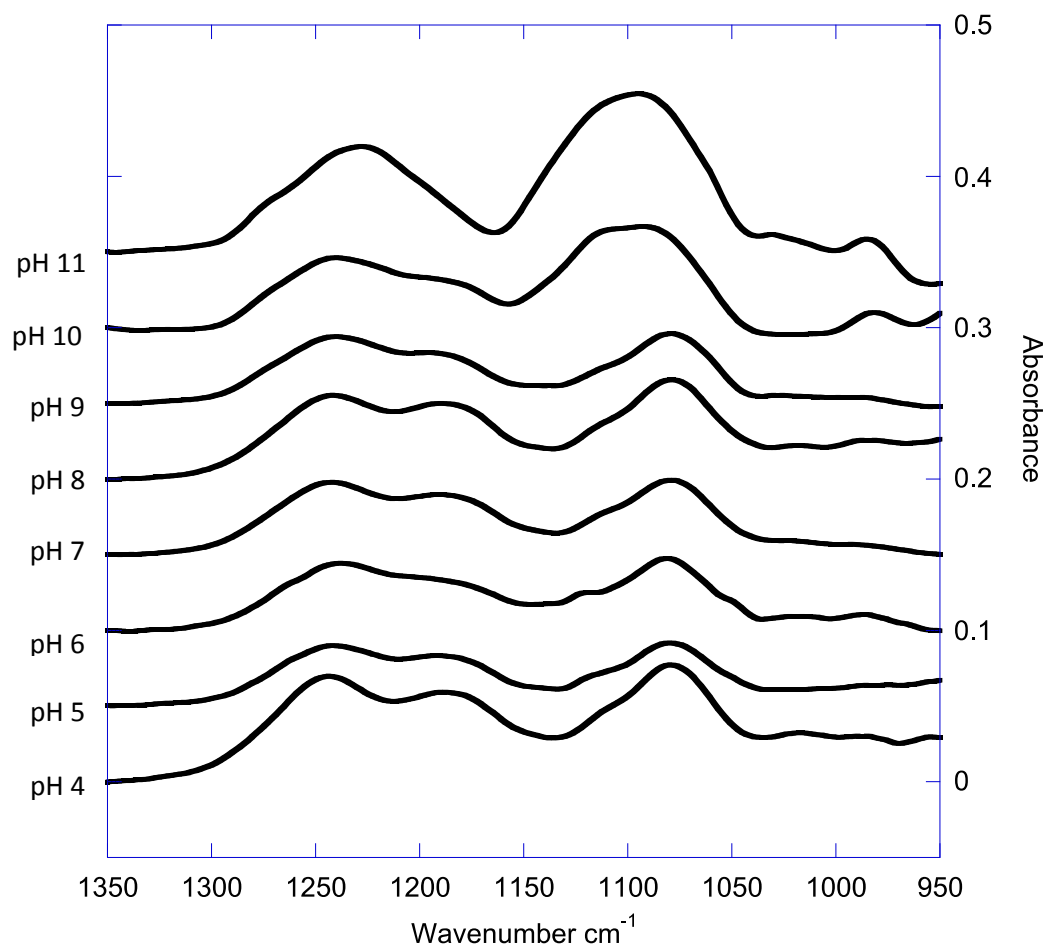


Figure 4: IR spectra ($950 - 1350 \text{ cm}^{-1}$) for multilamellar diacylglycerol pyrophosphate vesicles in the pH range 4 – 11. 20-50 mM Buffer (see for pH dependent details about the buffer the experimental section) and 100 mM NaCl. Final spectra were obtained by subtracting appropriate buffer spectra from the sample spectra. Spectra are smoothed with 17 smoothing points.

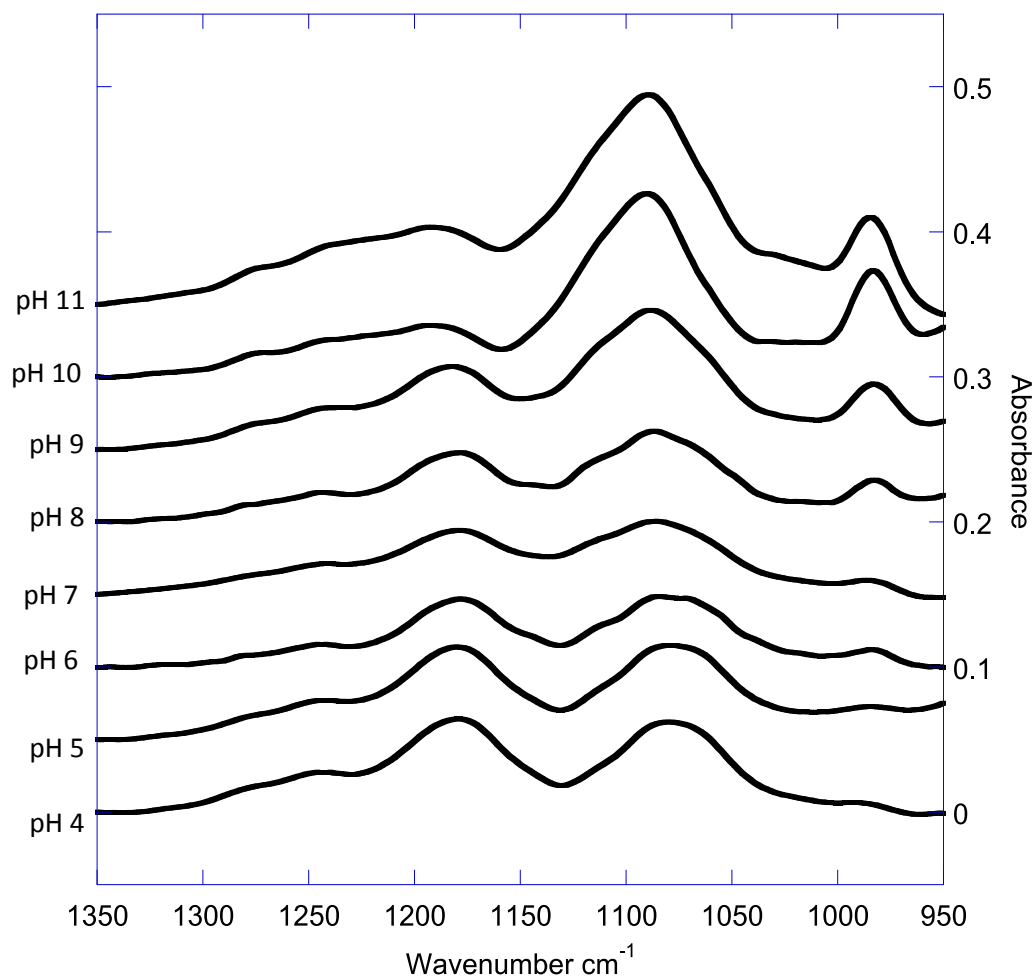


Figure 5: IR spectra ($950 - 1350 \text{ cm}^{-1}$) for multilamellar phosphatidic acid vesicles in the pH range 4 - 11. 20-50 mM Buffer (see for pH dependent details about the buffer the experimental section) and 100 mM NaCl. Final spectra were obtained by subtracting appropriate buffer spectra from the sample spectra. Spectra are smoothed with 17 smoothing points.

In order to best observe the trends of the phosphate group vibration bands in response to pH, the spectra of DGPP and DOPA are overlaid and presented collectively in Figure 4 and Figure 5, respectively. Individual spectra and their corresponding second derivatives are presented in the appendix.

For DGPP (Figure 4), weak bands are observed near 1280 cm^{-1} , 1245 cm^{-1} , 1020 cm^{-1} , and 985 cm^{-1} . Medium intensity bands are found near 1117 cm^{-1} , 1060 cm^{-1} . Strong bands are found near 1175 cm^{-1} , and 1088 cm^{-1} . The 1117 cm^{-1} and 985 cm^{-1} bands increase in intensity with rising pH, while the 1245 cm^{-1} and 1175 cm^{-1} bands decrease in intensity with rising pH. The remaining bands stay relatively constant throughout the experimental pH range.

For phosphatidic acid (Figure 5), weak bands are found near 1275 cm^{-1} , 1144 cm^{-1} (over pH 9), $1060\text{-}1047\text{ cm}^{-1}$, 1020 cm^{-1} , and 985 cm^{-1} . Medium intensity bands are found near 1190 cm^{-1} , 1175 cm^{-1} , and 1117 cm^{-1} . Strong bands are found near 1245 cm^{-1} , 1225 cm^{-1} , and 1080 cm^{-1} . The 1225 cm^{-1} , 1116 cm^{-1} , 1080 cm^{-1} , and 985 cm^{-1} bands increase in intensity with rising pH, while the 1245 cm^{-1} and 1175 cm^{-1} bands decrease with rising pH. The remaining bands remain relatively constant throughout the experimental pH range.

Discussion

Assignment of band positions

Table 1: Trends in peak position and strength of spectra produced by DGPP and DOPA. Numbers refer to wavenumber (cm⁻¹), (w) - weak peak, (m) - medium peak, (s) - strong peak.

DGPP								
pH 4	pH 5	pH 6	pH 7	pH 8	pH 9	pH 10	pH 11	Assignment
985 (w)	983 (w)	983 (w)	990 (w)	988 (w)	984 (w)	982 (m)	982 (m)	$\nu_s^\beta(\text{PO}_3^{2-})$
1020 (w)	1019 (w)	1016 (w)	1020 (w)	1018 (w)	1027 (w)	1028 (w)	1028 (w)	$\nu(\text{P-O})$ or $\nu(\text{C-O})$
		1047 (w)		1047 (w)	1065 (w)	1061 (w)	1061 (w/m)	$\nu_s^\alpha(\text{PO}_2^-)$, $\nu_s^\beta(\text{PO}_2^-)$
1077 (s)	1080 (s)	1080 (s)	1078 (s)	1084 (s)	1080 (s)	1085 (s)	1086 (s)	$\nu_s^\alpha(\text{PO}_2^-)/\nu_s^\beta(\text{PO}_2^-)/\nu_a(\text{PO}_3^{2-})$
1116 (m)	1117 (m)	1121 (m)	1115 (m)	1117 (w)	1116 (w)	1117 (s)	1118 (s)	$\nu_a^\beta(\text{PO}_2^-)$, $\nu_a^\beta(\text{PO}_3^{2-})$
					1144 (w)	1143 (w)	1143 (w)	$\nu_a^\beta(\text{PO}_3^{2-})$
1175 (m/s)	1175 (m/s)	1176 (m/s)	1173 (m/s)	1178 (m/s)	1179 (m)	1178 (w/m)	1179 (w)	$\nu_a^\beta(\text{PO}_2^-)$
1184 (m/s)			1193 (m/s)					Cannot yet assign
		1230 (s)				1222 (w)	1222 (s)	$\nu_s^\alpha(\text{PO}_2^-)$, $\nu_s^\beta(\text{PO}_2^-)$
1245 (s)	1242 (s)		1244 (s)	1245 (m/s)	1244 (s)	1244 (s)	1244 (m)	$\nu_s^\alpha(\text{PO}_2^-)$, $\nu_s^\beta(\text{PO}_2^-)$
		1263 (w)						
					1274 (w)	1276 (w/m)	1276 (w/m)	$\nu(\text{C-O})?$
DOPA								
pH 4	pH 5	pH 6	pH 7	pH 8	pH 9	pH 10	pH 11	Assignment
989 (w)	985 (w)	983 (m)	982 (m)	983 (m)	983 (s)	984 (s)	984 (s)	$\nu_s(\text{PO}_3^{2-})$
1020 (w)		1019 (w)		1018 (m)	1020 (w)	1020 (w)	1025 (w)	$\nu(\text{P-O})$ or $\nu(\text{C-O})$
1063 (m)	1063 (m)	1060 (m)	1062 (m)	1059 (m)	1058 (m)			$\nu_s(\text{PO}_2^-)$
1088 (s)	1088 (s)	1087 (s)	1087 (s)	$\nu_s(\text{PO}_2^-)/\nu_a(\text{PO}_3^{2-})$				
	1116 (w)	1117 (m)	1116 (m)	1117 (m)	1117 (m)	1117 (m)		$\nu_a(\text{PO}_3^{2-})$
1175 (s)	1175 (s)	1175 (s)	1175 (s)	1174 (s)	1175 (s)	1175 (m)	1177 (m)	$\nu_a(\text{PO}_2^-)$
1246 (m)	1246 (m)	1245 (m)	1247 (m)	1244 (m)	1245 (m)	1245 (m)	1244 (m)	$\nu_s(\text{PO}_2^-)$
1282 (w)	1281 (w)	1280 (w)	1282 (w)	1280 (w)	1279 (w)	1278 (w)	1277 (w)	$\nu(\text{C-O})?$

Due to the overlapping nature of many bands in the wavenumber range of interest for this study (1350-950 cm⁻¹), band assignments can sometimes be subject to controversy and uncertainty. In the background, the MMP characterization and band assignment was useful for determining what wavenumber range to expect particular vibrational modes at with respect to changes in pH, and aided with certain band assignments. Additionally, utilization of past publications (Barth, 1995, 1998; Shimanouchi, 1960) has led to reasonable certainty in the following proposed band assignments, and are in agreement with all three of the mentioned studies unless otherwise noted. Those band

assignments which are not agreed upon between the three studies will be discussed accordingly. When necessary, the distinction between vibrational modes of the phosphomonoester and phosphodiester groups of DGPP will be made clear. Table 1 gives an overview of the trends of band position, intensity,

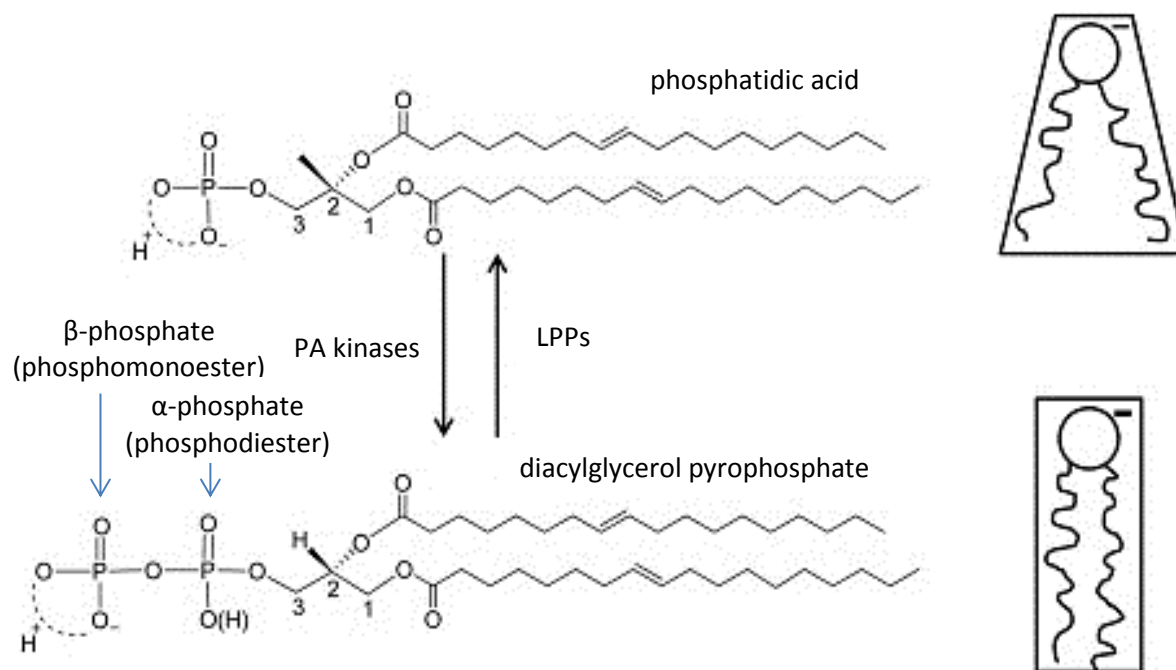


Figure 6: Structure and functional model for DGPP. On the left the chemical structures of DOPA (top) and DGPP (bottom) are shown. For DGPP, the α -phosphate (phosphodiester) and β -phosphate (phosphomonoester) groups are indicated. On the right the effective molecular shapes of PA and DGPP at physiological pH and salt (NaCl) concentration are shown.

and assignment for DOPA and DGPP.

To begin with the highest wavenumber and the assignment mentioned only in the Barth 1998 study, it is proposed that the band near $1275\text{-}1280\text{ cm}^{-1}$ for both lipids results from $\nu(\text{C-O})$. This assignment seems reasonable, since the weak band is detectable across the entire experimental pH range at a relatively constant intensity, indicating the independency of this vibrational mode to pH. Next, the following bands are assigned to $\nu_a(\text{PO}_2^-)$ stretching: 1245 cm^{-1} (Barth, 1995), 1225 cm^{-1} (Barth, 1998; Shimanouchi, 1960), and $1185\text{-}1175\text{ cm}^{-1}$ (Barth, 1995; Shimanouchi, 1960). In DOPA, the 1245 cm^{-1} band is relatively weak and appears to stay relatively constant, the 1175 cm^{-1} band starts strong and gradually decreases in intensity as pH increases, and the 1225 cm^{-1} band is not observed. In contrast, all

of these bands are observed in the DGPP spectra, but each must be attributed to either the phosphomonoester or phosphodiester group. DGPP exhibits two phosphate groups, shown in the model of Figure 6: The phosphodiester group of the α -phosphate that is expected to be invariant throughout the investigated pH range since the pK_a for the dissociation of the proton is found somewhere around pH 2. Therefore, we expect to find symmetric and asymmetric $\nu(\text{PO}_2^-)$ stretching vibrations that are associated with this group. The β -phosphate is single negatively charged at the starting pH and becomes increasingly deprotonated as the pH is being raised. Therefore, initially the spectra will exhibit bands that are characteristic for a $\text{P}(\text{OH})\text{O}_2^-$ group, which are being transformed into bands that are characteristic for a PO_3^{2-} group. Since the phosphodiester group of DGPP cannot deprotonate to the PO_3^{2-} species, any PO_2^- band which decreases in intensity with rising pH must result from the phosphomonoester group, and PO_2^- bands which maintain a constant intensity must result from the phosphodiester group. For DGPP, the proposed assignment of $\nu_a(\text{PO}_2^-)$ stretching corresponds to 1248 cm^{-1} and 1225 cm^{-1} for the phosphodiester group and $1180\text{--}1175\text{ cm}^{-1}$ for the phosphomonoester group.

The following bands are assigned to $\nu_s(\text{PO}_2^-)$: 1115 cm^{-1} (Barth 1995, 1998), $1088\text{--}1077\text{ cm}^{-1}$ (Barth, 1995, 1998; Shimanouchi, 1960), and 1060 cm^{-1} (Barth, 1995; Shimanouchi, 1960). For DOPA, these are all due to phosphomonoester stretching, but since these bands are all relatively close, it is difficult to determine the exact trends each one expresses, especially since the strong peak near 1090 cm^{-1} develops at higher pH values but is discussed later as a PO_3^{2-} band. For DGPP, the band near 1115 cm^{-1} is likely due to antisymmetric stretching of the phosphomonoester group, since a peak is present at low pH, which grows as a PO_3^{2-} band at higher pH, whereas the band near 1080 cm^{-1} is likely due to antisymmetric phosphodiester stretching band since this band does not change in intensity in response to pH. The weak band at 1060 cm^{-1} is difficult to assign a trend for because of the nearby strong band, and cannot be assigned with certainty to one phosphate group or the other.

The bands corresponding to the $\nu_a(\text{PO}_3^{2-})$ stretching bands are 1143 cm^{-1} (Barth, 1998), 1115 cm^{-1} (Barth, 1995, 1998) and 1088 cm^{-1} (Barth, 1995). Since the phosphodiester group of DGPP cannot deprotonate to the PO_3^{2-} species, all PO_3^{2-} related vibrational modes are due to the phosphomonoester group (β -phosphate). The 1143 cm^{-1} band is interesting because it is only starting to develop at pH 9 as a very weak band, likely a shoulder of the stronger peaks close by at near 1115 cm^{-1} . Though the weak 1115 cm^{-1} band is attributed to $\nu_s(\text{PO}_2^-)$ at lower pH values, its rapid increase in intensity between pH 9 and 10 clearly points to its assignment as $\nu_a(\text{PO}_3^{2-})$. This band reaches approximately a 1:1 ratio with the nearby $1088\text{--}1077\text{ cm}^{-1}$, the upper wavenumber range of which is likely attributable to $\nu_a(\text{PO}_3^{2-})$ stretching, since the peak shifts from 1077 cm^{-1} to 1088 cm^{-1} between pH 4 and 11. The bands which appear to correspond to $\nu_s(\text{PO}_3^{2-})$ are found near 1060 cm^{-1} and 985 cm^{-1} . In DOPA, it is likely that the only band corresponding to this species is the 985 cm^{-1} band, since the spectra indicate, if anything, a decrease in the intensity of the 1060 cm^{-1} band. In DGPP, the 1060 cm^{-1} band, while it is present more as a shoulder of the 1088 cm^{-1} peak, still clearly increases with rising pH. Additionally, the 985 cm^{-1} band is attributed to $\nu_s(\text{PO}_3^{2-})$, but does not produce as strong a peak as DOPA does when the spectra of equivalent pH are compared. This difference between the trends of similar band assignments of the two spectra will be discussed later.

The remaining band at 1020 cm^{-1} for both lipids is given the assignment of $\nu(\text{P-O})$ stretching (Barth, 1995). A level of uncertainty comes with this assignment since it is only mentioned in one of the studies, and appears as a very weak shoulder of a nearby stronger peak.

Implications for the Ionization of PA and DGPP

As mentioned earlier, DGPP is expected to carry a greater negative charge than DOPA at comparable pH due to its pyrophosphate head group. The data presented in this study indicates that when DGPP is examined by itself (i.e., not in a mixture with another lipid) this is not true. While the

symmetric and asymmetric PO_3^{2-} bands for DOPA begin increasing in intensity starting even at pH 7, the same bands for DGPP do not clearly increase until pH 10. Discussed in the introduction, it was hypothesized that the phosphomonoester of DGPP penetrates farther from the membrane towards the aqueous phase, experiencing a larger dielectric constant, and a lowering of its $\text{pK}_{\text{a}2}$. Since DGPP was not examined in a membrane environment for this study, the reason that DGPP did not acquire the larger negative charge before DOPA is possibly due to shielding of the phosphomonoester by the phosphodiester. That is, because there is only one phosphate group on DOPA, that phosphate group is the only group in the zone of interest in this study to change in ionization. In contrast, the two phosphate groups of DGPP likely have a less straightforward ionization pattern. It would seem that the phosphodiester PO_2^- group is able to blunt the deprotonation of the phosphomonoester group until approximately pH 10. Referring to the initial expectation, it is likely that when the DGPP phosphomonoester is penetrating into the membrane it would be able to ionize as without this effect from the phosphodiester. Strawn et al. confirmed that the $\text{pK}_{\text{a}2}$ of DPA is around pH 7.9 compared to the much lower pH 7.4 of DGPP in a DOPC membrane (2012). Strawn et al. also analyzed the charge on the phosphodiester of DGPP in response to pH, and observed that its position does not change significantly compared to the phosphomonoester. It is proposed that it is likely that the shift of the phosphodiester is due solely to the decrease in shielding of the phosphomonoester group because of the deprotonization in response to rising pH. Strawn et al. further propose that since the phosphodiester of DGPP has a similar $\text{pK}_{\text{a}1}$ to PA, it is unlikely for the phosphomonoester and phosphodiester to deprotonate simultaneously. In conclusion, the higher than expected $\text{pK}_{\text{a}2}$ for the β -phosphate might be due to intra- or intermolecular hydrogen bond formation where the proton of the phosphomonoester group is shared with a phosphodiester group. Such an interaction would increase the $\text{pK}_{\text{a}2}$.

Conclusions

Previous studies (e.g. Strawn et al., 2012) concluded that in biological membranes, DGPP is likely to carry a more negative charge than PA, because of its additional phosphate group and its ability to penetrate further from the membrane. It was proposed then that both the charge and packing properties of DGPP worked together in turning off the PA signal. Villasuso et al. indicated that the surface behavior of individual lipids DGPP and PA can be changed by varying the proportions of each lipid, which showed their capability for inducing membrane events through variations of molecular packing, in-plane elasticity, and electrostatic interactions.

The findings of this study suggest that pure DOPA multilamellar vesicles deprotonate to the PO_3^{2-} species at lower pH levels than the phosphomonoester group of DGPP multilamellar vesicles deprotonate to the PO_3^{2-} species. While this does not necessarily mean that DOPA carries a larger negative charge (single-deprotonated DGPP has a charge of 2-; at best PA can reach an equivalent charge), it does have potential implications for protein binding. Since Strawn et al. found that in a DOPC membrane DGPP has a smaller pK_a_2 than DOPA, it is likely that in certain biological scenarios DGPP will have a more negative charge than PA, as discussed previously. However, the findings presented in this study help to expand the small pool of what is known about DGPP with the intention of discerning what it actually does in biological systems and how it exerts its effects.

Although the overall molar concentration of DGPP in biological membranes is low, its local concentration at specific sites may be significantly higher. It is not yet known exactly what type of signaling involving PA might trigger the local increase of DGPP. A better understanding of the properties of the enzymes that control DGPP's biological concentrations is important in understanding its role. Cloning the PAK encoding gene would help identify *PAK* genes in other plants, and reverse genetics should be used to alter expression of PAK and DPP genes to examine their effects on growth and

development. Additionally, isolation and characterization of DGPP-binding proteins is important; if these included recognized signaling proteins, DGPP would be established as a second messenger.

References

- Cevc, G. 1990. Membrane electrostatics. *Biochim. Biophys. Acta* 1031:311-382.
- Darwish, E., C. Testerink, M. Khalil, O. El-Shihy, and T. Munnik. 2009. Phospholipid signaling responses in salt-stressed rice leaves. *Plant Cell Physiol.* 50:986-997.
- Dawson, J. E. 2002. Infrared spectroscopic analysis of inositol phosphates: assignment of vibrational modes. In Chemistry. Kent State University. 49.
- de Jong, C. F., A. M. Laxalt, B. O. d. W. Bargmann, P.J., M. H. Joosten, and T. Munnik. 2004. Phosphatidic acid accumulation is an early response in the Cf-4/Avr4 interaction. *Plant J.* 39:1-12.
- den Hartog, M., A. Musgrave, and T. Munnik. 2001. Nod factor-induced phosphatidic acid and diacylglycerol pyrophosphate formation: a role for phospholipase C and D in root hair deformation. *Plant J.* 25:55-65.
- den Hartog, M., N. Verhoef, and T. Munnik. 2003. Nod factor and elicitors activate different phospholipid signaling pathways in suspension-cultured alfalfa cells. *Plant Physiol.* 132:311-317.
- Dillon, D. A., W. I. Wu, B. Riedel, J. B. Wissing, W. Dowhan, and G. M. Carman. 1996. The *Escherichia coli* pgpB gene encodes for a diacylglycerol pyrophosphate phosphatase activity. *J. Biol. Chem.* 271:30548-30553.
- Gennis, R. B. 1989. Biomembrane, Molecular Structure and Function. Springer-Verlag, New York.
- Jeannette, E., S. Paradis, and C. Zalejski. 2010. In Lipid Signaling in Plants. T. Munnik, editor. Springer-Verlag, Berlin. 263-276.
- Katagiri, T., K. Ishiyama, T. Kato, S. Tabata, M. Koboyashi, and K. Shinozaki. 2005. An important role of phosphatidic acid in ABA signaling during germination in *Arabidopsis thaliana*. *Plant J.* 43:107-117.
- Ktistakis, N. T., C. Delon, M. Manifava, E. Wood, I. Ganley, and J. M. Sugars. 2003. Phospholipase D1 and

- potential targets of its hydrolysis product, phosphatidic acid. *Biochem. Soc. Trans.* 31:94-97.
- Latijnhouwers, M., T. Munnik, and F. Govers. 2002. Phospholipase D in *Phytophthora infestans* and its role in zoospore encystment. *Mol. Plant-Microb. Interact.* 15:939-946.
- Marsh, D. 2012. Handbook of Lipid Bilayers. CRC Press, Boca Raton, FL.
- Munnik, T., H. J. Meijer, B. Ter Riet, H. Hirt, W. Frank, D. Bartels, and A. Musgrave. 2000. Hyperosmotic stress stimulates phospholipase D activity and elevates the levels of phosphatidic acid and diacylglycerol pyrophosphate. *Plant J.* 22:147-154.
- Pical, C., T. Westergren, S. K. Dove, C. Larsson, and M. Sommarin. 1999. Salinity and hyperosmotic stress induce rapid increases in phosphatidylinositol 4,5-bisphosphate, diacylglycerol pyrophosphate, and phosphatidylcholine in *Arabidopsis thaliana* cells. *J. Biol. Chem.* 274:28232-28240.
- Pierrugues, O., C. Brutescio, J. Oshiro, M. Gouy, Y. Deveaux, G. M. Carman, P. Thuriaux, and M. Kazmaier. 2001. Lipid phosphate phosphatases in *Arabidopsis*. Regulation of the AtLPP1 gene in response to stress. *J. Biol. Chem.* 276:20300-20308.
- Redfern, D. A., and A. Gericke. 2004. Domain Formation in Phosphatidylinositol Monophosphate/Phosphatidylcholine Mixed Vesicles. *Biophysical J.* 86:2980-2992.
- Rizzo, M., and G. Romero. 2002. Pharmacological importance of phospholipase D and phosphatidic acid in the regulation of the mitogen-activated protein kinase cascade. *Pharmacol. Ther.* 94:35-50.
- Roth, M. G. 2008. Molecular mechanisms of PLD function in membrane traffic. *Traffic* 9:1233-1239.
- Seelig, J. 1997. Titration calorimetry of lipid-peptide interactions. *Biochimica et Biophysica Acta* 1331:103-116.
- Shimanouchi, T., M. Tsuboi, and Y. Kyogoku. 1964. Infrared Spectra of Nucleic Acids and Related Compounds. In *Advances in Chemical Physics. The Structure and Properties of Biomolecules and Biological Systems*. Interscience Publishers, Great Britain. 467.
- Stace, C. L., and N. T. Ktistakis. 2006. Phosphatidic acid- and phosphatidylserine-binding proteins.

- Biochim. Biophys. Acta* 1761:913-926.
- Strawn, L., A. Babb, C. Testerink, and E. E. Kooijman. 2012. The physical chemistry of the enigmatic phospholipid diacylglycerol pyrophosphate. *Frontiers in Plant Science* 3:9.
- Testerink, C., and T. Munnik. 2011. Molecular, cellular, and physiological responses to phosphatidic acid formation in plants. *J. Exp. Bot.* 62:2349-2361.
- Thomas, L. C., and R. A. Chittenden. 1964. *Spectrochim. Acta* 20:467-487.
- Thomas, L. C., and R. A. Chittenden. 1970. *Spectrochim. Acta* 26A:781-790.
- Tocanne, J. F., and J. Teissie. 1990. Ionization of phospholipids and phospholipid-supported interfacial lateral diffusion of protons in membrane model systems. *Biochim. Biophys. Acta* 1031:111-142.
- Toke, D. A., W. L. Bennett, D. A. Dillon, W. I. Wu, X. Chen, D. B. Ostrander, J. Oshiro, A. Cremesti, D. R. Voelker, A. S. Fischl, and G. M. Carman. 1998. Isolation and characterization of the *Saccharomyces cerevisiae* DPP1 gene encoding diacylglycerol pyrophosphate phosphatase. *J. Biol. Chem.* 273:3278-3284.
- Toke, D. A., W. L. Bennett, J. Oshiro, W. I. Wu, D. R. Voelker, and G. M. Carman. 1998. Isolation and characterization of the *Saccharomyces cerevisiae* LPP1 gene encoding a Mg²⁺-independent phosphatidate phosphatase. *J. Biol. Chem.* 273:14331-14338.
- Tsuboi, M. 1957. *J. Am. Chem. Soc.* 79.
- van der Luit, A. H., T. Piatti, A. van Doorn, A. Musgrave, G. Felix, T. Boller, and T. Munnik. 2000. Elicitation of suspension-cultured tomato cells triggers the formation of phosphatidic acid and diacylglycerol pyrophosphate. *Plant Physiol.* 123:1507-1516.
- van Schooten, B., C. Testerink, and T. Munnik. 2006. Signalling diacylglycerol pyrophosphate, a new phosphatidic acid metabolite. *Biochimica et Biophysica Acta* 1761:151-159.
- Villasuso, A. L., N. Wilke, M. Bruno, and E. Machado. 2010. The surface organization of diacylglycerol pyrophosphate and its interaction with phosphatidic acid at the air-water interface. *Chemistry*

and Physics of Lipids 163:771-777.

Zalejski, C., S. Paradis, R. Maldiney, Y. Habricot, E. Miginiac, J. P. Rona, and E. Jeanette. 2006. Induction of abscisic acid-regulated gene expression by diacylglycerol pyrophosphate involves Ca²⁺ and anion currents in *Arabidopsis thaliana* suspension cells. *Plant Physiol.* 141:1555-1562.

Zalejski, C., Z. Zhang, A. L. Quettier, R. Maldiney, M. Bonnet, M. Brault, C. Demandre, E. Miginiac, J. P. Rona, B. Sotta, and E. Jeannette. 2005. Diacylglycerol pyrophosphate is a second messenger of abscisic acid signaling in *Arabidopsis thaliana* suspension cells. *Plant J.* 42:145-152.

Appendix

